AN IMPROVED PIXON-BASED APPROACH FOR IMAGE SEGMENTATION

H. Hassanpour*

School of Computer Engineering & IT, Shahrood University of Technology
Shahrood, Iran, h_hassanpour@yahoo.com

H. Yousefian

Department of Electrical Engineering, Iran University of of Science and Technology (IUST)
Tehran, Iran, hadi_yousefian18@yahoo.com

*Corresponding Author

(Received: June 29, 2009 – Accepted in Revised Form: March 11, 2010)

Abstract An improved pixon-based method is proposed in this paper for image segmentation. In this approach, a wavelet thresholding technique is initially applied on the image to reduce noise and to slightly smooth the image. This technique causes an image not to be oversegmented when the pixon-based method is used. Indeed, the wavelet thresholding, as a pre-processing step, eliminates the unnecessary details of the image and results in a fewer pixon number, faster performance and more robustness against unwanted environmental noises. The image is then considered as a pixonal model with a new structure. The obtained image is segmented using the hierarchical clustering method (Fuzzy C-Means algorithm). The experimental results in this paper indicate that the proposed pixon-based approach has a reduced computational load and a better accuracy compared to the other existing image segmentation techniques.

Keywords Image segmentation, Pixon, Wavelet thresholding

چکیده در این مقاله یک روش مبتنی بر پیکسل برای قطعه بندی تصویر ارائه می‌شود. در این روش، به منظور کاهش اثر نویز و هموار سازی مختصر تصویر، ابتدا تکنیک آستانه گذاری موجک بر روی تصویر اعمال می‌شود. این تکنیک مانع از سگمنت شدن بیش از حد تصویر هنگام استفاده از پیکسل میگردد. در واقع، آستانه گذاری موجک، به عنوان یک مرحله پیش پردازش، جزئیات غیر ضروری تصویر را حذف می‌نماید و به موجب آن تعداد پیکسون کاهش، کارایی افزایش و پایداری آن در مقابل نویزهای محیطی افزایش می‌یابد. سپس تصویر مورد نظر با یک ساختار جدید در یک مدل پیکسونی ارائه میگردد. تصویر حاصل با استفاده از روش خوشه بندی سلسله مراتبی (الگوریتم فازی C-Means) قطعه بندی می‌شود. نتایج تجربی در این تحقیق نشان میدهد که روش مبتنی بر پیکس ارائه شده در این مقاله، در مقایسه با سایر روشهای قطعه‌بندی تصویر، دارای بار محاسباتی کمتر و دقت بهترمی‌باشد.

1. INTRODUCTION

Image segmentation is a process of partitioning image into several disjoint regions with similar characteristics in terms of intensity, color and texture. It has wide applications in image processing and is often employed as a pre-processing stage in various applications such as mobile object tracking, medical imaging and face recognition [1].

A considerable number of segmentation techniques exist in the literature. These techniques can be classified in several groups; thresholding-based methods, which determine threshold values using the image histogram and then classify the image pixels based on these values [2]; region-based methods, which group pixels into homogeneous regions and segment the image to some major areas, such as region growing [3, 4]; clustering-based methods, which segment the feature space of image to several clusters and get a sketch of the original image, such as K-means [5], Fuzzy C-Means (FCM) [6] and mean-shift [7] algorithms. Modeling images with Markov Random Fields (MRF) is another approach which has been recently developed to segment images [8-10]. To achieve this purpose, these methods try to minimize the energy function of image using clique concept and Gibbs distribution. However, the main disadvantage of MRF-based methods is

that the minimization problem of objective function is very time consuming in these algorithms. Recently the pixon-based approaches for image segmentation have received considerable attention among the researchers. The pixon concept, initially introduced in [11] and later in [12], is a set of disjoint regions with constant shapes and variable sizes. In this concept, the pixon definition scheme is a local convolution between a kernel function and a pseudo image. The drawback of this scheme is that the shape of the pixons can not vary once the kernel function is selected. However, both the shape and size of the pixons can vary if the definition scheme introduced in [13] is used. In this scheme, the anisotropic diffusion equation is used to form the pixons. Then the MRF concept is considered in segmenting the images. Recently, another pixon-based image segmentation was introduced in [14]. In this approach, the pixons combined with their attributes and adjacencies construct a graph, which represents the observed image. This technique uses a fast QuadTree combination (FQTC) algorithm to extract a good pixon-representation. These techniques integrated into MRF model and resulted in a faster performance in comparison with the previous approaches, as reported in [14].

For the technique proposed in this paper, first a pre-processing step is performed which applies the wavelet thresholding technique. This step due to the noise reduction property of wavelet thresholding is suitable for image smoothing. To avoid over-smoothing problem, the value of the threshold must be assigned properly. Then, the pixon-based algorithm is used to form and extract the pixons. The advantage of using pixons is that after forming the pixons the decision level changes from pixels to pixons and this decreases the computational time, because of the fewer number of pixons compared to the number of pixels. Finally, the Fuzzy C-Means (FCM) algorithm is applied to segment the image.

The results of applying the proposed method on several standard images show that by incorporating wavelet thresholding followed by the pixon concept, the number of pixons and consequently the computational time can be decreased significantly and the presented method excel in some criteria such as variance and pixon to pixel ratio compared to other existing approaches.

The rest of the paper is organized as follows: the pixon concept is described in the next section. This is followed by the proposed method in Section 3 which includes the pre-processing step and the use of pixon concept for image segmentation. The experimental results obtained using our technique on a variety of image data are presented in Section 4. We conclude the paper in Section 5.

2. DESCRIPTION OF PIXON SCHEME

The main idea of the pixon concept is that at each point in the image there is a finest spatial scale of interest and that there is no information content below this scale. The size, shape and position of all pixons over an image can be collected into a pixon map, which gives an adaptive scale description of the image with various spatial scales. Since different parts of an image often do not exhibit a uniform spatial resolution, the pixon map, as an adaptive scale representation language, suggests itself. It gives the finest spatial scale at each portion of the image [13].

The fuzzy pixon definition scheme for astronomical image restoration and reconstruction was proposed in [11]. In this scheme, the image is modeled by a local convolution of a pseudo- image and a kernel function. At each pixel, the image is written as below:

$$Y(t) = \left(K \otimes I_p\right) = \int K_t(t,v) I_p(v) dv \qquad (1)$$

where $K_t(t,v)$ is the pixon kernel function. In the fuzzy pixon definition scheme, once a pixon kernel function is selected, the pixon is completely determined by its size. Hence, the pixon shape does not vary and only the pixon size can change according to the observed image. By picking a set of pixons, a pixon map gives an adaptive scale description of the image.

Later, a novel pixon definition scheme was presented in [13] which can be described as follows

$$I_p = \bigcup_{j=1}^{m} P_j \qquad (2)$$

where I_p is the pixon-based image model, m is the

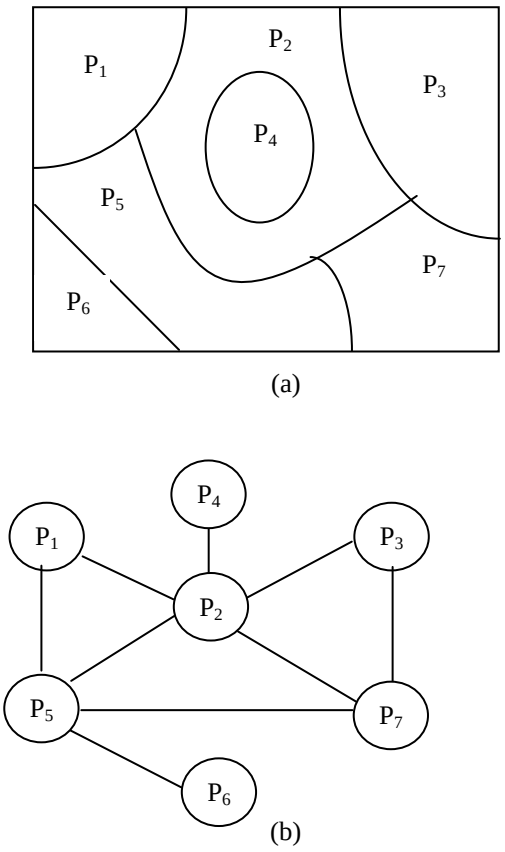

Figure 1. (a) Pixon model of image, and (b) the corresponding graph structure.

number of pixons, Pj is a pixon which is made up of a set of connected pixels, a single pixel or even a sub-pixel. The mean value of the connected pixels making up of the pixon is defined as the pixon intensity. Both the shape and size of each pixon can vary according to the observed image. After the pixon-based image model is defined, the image segmentation problem is transformed into a problem of labeling pixons.

To form the pixons, the researchers first obtained a pseudo-image which had at least the same resolution as the main image and then used an anisotropic diffusion filter for formulation of the pixons. Eventually they used a segmentation method to extract the pixons.

The pixon-based image model is represented by a graph structure $G = (Q, E)$, where Q is the finite set of vertices of the graph and E is the set of edges of the graph (Figure 1).

The authors in [14] introduced a pixon representation technique and used the FQTC algorithm to extract the pixons. They defined an attribute vector for each pixon

$$\overrightarrow{P_i} = (n_i, b_i, max_i, min_i, \mu_i, {\sigma_i}^2) \quad (3)$$

where n_i is the number of pixels in P_i , b_i is the perimeter of P_i, and max_i, min_i, μ_i and ${\sigma_i}^2$ are the maximum, minimum, mean and variance of the observed image intensities in P_i, respectively. In their definition, a function $f(p) \geq 0$ of pixons is a pixon error function and the edge error function is defined as $f_E(E_{i,j}) = f(P_i \oplus P_j)$ which $P_i \oplus P_j$ implies the combination of P_i and P_j . To extract a good pixon-representation with a given non-negative constant, T, the pixons connected by the edge with the minimal edge error are combined iteratively until the minimal edge error is larger than T.

3. PROPOSED METHOD

3.1 Pre-Processing Step As mentioned above, we use the wavelet thresholding technique as a pre-processing step to smooth the image. For this purpose, by choosing an optimal wavelet level and an appropriate mother wavelet, the image is decomposed into different channels, namely low-low, low-high, high-low and high-high (LL, LH, HL, HH respectively) channels and their coefficients are extracted in each level. The decomposition process can be recursively applied to the low frequency channel (LL) to generate decomposition at the next level. The suitable threshold value is selected using an existing thresholding methods [15-17] and then details coefficients are cut using this threshold. Afterward, inverse wavelet transform is performed and the smoothed image is reconstructed.

3.1.1 Wavelet Thresholding Technique

Thresholding is a simple non-linear technique which operates on the wavelet coefficients. In this technique, each coefficient is passed through the threshold function. The coefficients which are smaller than the threshold are set to zero and the others are kept or modified by considering the

thresholding method. Whereas the wavelet transform is good for energy compaction, the small coefficients are considered as noise and large coefficients indicate important signal features [18]. Therefore, these small coefficients can be cut with no effect on the significant features of the image.

Let $X = \{X_{i,j},\ i,j = 1,2 \ldots M\}$ denotes the $M \times M$ matrix of the original image. The two dimensional orthogonal Discrete Wavelet Transform *(DWT)* matrix and its inverse are implied by W and W^{-1}, respectively. After applying the wavelet transform to the image matrix *X*, this matrix is subdivided into four sub-bands namely *LL*, *HL*, *LH* and *HH* [18, 19].

Whereas the *LL* channel possesses the main information of the image, we apply the hard or soft thresholding technique to the other three sub-bands which contain the details coefficients. The outcome matrix which is produced after utilizing the thresholding level is denoted as $\hat{L}$. Finally, the smoothed image matrix can be obtained as follows:

$$\hat{X} = W^{-1}\,\hat{L} \tag{4}$$

The brief description of the hard thresholding is as follows:

$$\gamma(Y) = \begin{cases} Y & if\ \ |Y| > T \\ 0 & otherrwise \end{cases} \tag{5}$$

where Y is an arbitrary input matrix, $\gamma(Y)$ is the hard thresholding function applied on Y, and T indicates the threshold value. Using this function, all coefficients less than the threshold are replaced with zero and other coefficients are kept unchanged.

The soft thresholding acts similar to the hard one, except that in this method the values above the threshold are reduced by the threshold value. The following equation implies the soft thresholding function:

$$\eta(Y) = \begin{cases} sign(Y)(|Y| - T)\ \ if\ \ |Y| > T \\ 0 \qquad\qquad\qquad otherrwise \end{cases} \tag{6}$$

where Y is the arbitrary input matrix, $\eta(Y)$ is the soft thresholding function and T indicates the threshold value. Our research indicates that the soft thresholding method is more desirable in comparison with the hard thresholding because of its better visual performance. The hard thresholding method may cause some discontinuous points in the image and this event may be a discouraging factor for the performance of our segmentation.

Three methods have been presented in the literature to calculate the threshold value, namely Visushrink, Bayesshrink and Sureshrink [15-17]. Visushrink is based on applying the universal threshold proposed in [15]. This thresholding is given by $\sigma\sqrt{2logM}$ where σ is standard deviation of noise and M is the number of pixels in the image. This threshold does not adapt well with discontinuities in the image. SureShrink is also a practical wavelet procedure, but it uses a local threshold estimated adaptively for each level [16]. The Bayesshrink rule uses a Bayesian mathematical framework for images to derive subband-dependent thresholds. These thresholds are nearly optimal for soft thresholding, because the wavelet coefficients in each subband of a natural image can be summarized adequately by a generalized Gaussian distribution (GGD) [17].

3.1.2 Algorithm and results

Our implementations on several different types of images show that *Daubechies* is one of the most suitable wavelet filters for this purpose. An image is decomposed, in our case, up to 2 levels using *8-tap Daubechies* wavelet filter. The amount of the threshold is assigned by the *Bayesshrink* rule and this value may be different for each image. This algorithm can be expressed as follows. First image is decomposed into four different channels, namely LL, LH, HL and HH. Then the soft thresholding function is applied on these channels, except on LL. Finally the smoothed image is reconstructed by inverse wavelet transform. Figure 2 shows the result of applying wavelet thresholding on the Baboon image. It can be inferred from this figure that the resulted image has fewer discontinuities than the original image and its smoothing degree improved which results in a fewer number of pixons.

3.2 Pixonal Image Segmentation As mentioned before, we present an improved method to segment the image. In this approach the wavelet thresholding technique is used as a pre-processing step to make the image smoothed. This technique is applied on the wavelet transform coefficients of image using the soft thresholding function.

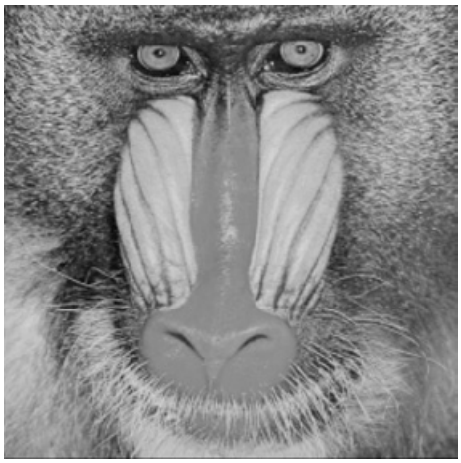

(a)

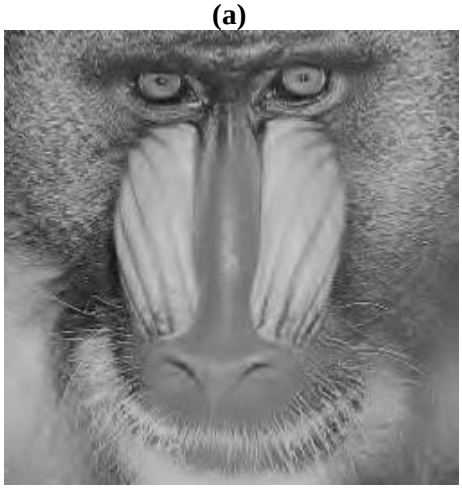

(b)

Figure 2. Result of applying wavelet thresholding technique on Baboon image: (a) Original image, and (b) smoothed image.

The output of pre-processing step is then used in the pixon formulation stage. In Yang's pixon-based algorithm, after obtaining the pseudo image, the anisotropic diffusion equation was used to form the pixons. In our proposed algorithm, utilizing the wavelet thresholding method as a pre-processing stage eliminates the necessity of using the diffusion equations. After forming and extracting the pixons, the Fuzzy C-Means (FCM) algorithm is used to segment the image. The FCM algorithm is an iterative procedure described in the following [20]:

Given M input data $\{x_m; m = 1,\ldots,M\}$, the number of clusters C $(2 \le C < M)$, and the fuzzy weighting exponent $w, 1 < w < \infty$, initialize the fuzzy membership functions $u^{(0)}{}_{c,m}$ with $c = 1,\ldots,C$ and $m = 1,\ldots,M$ which are the entry of

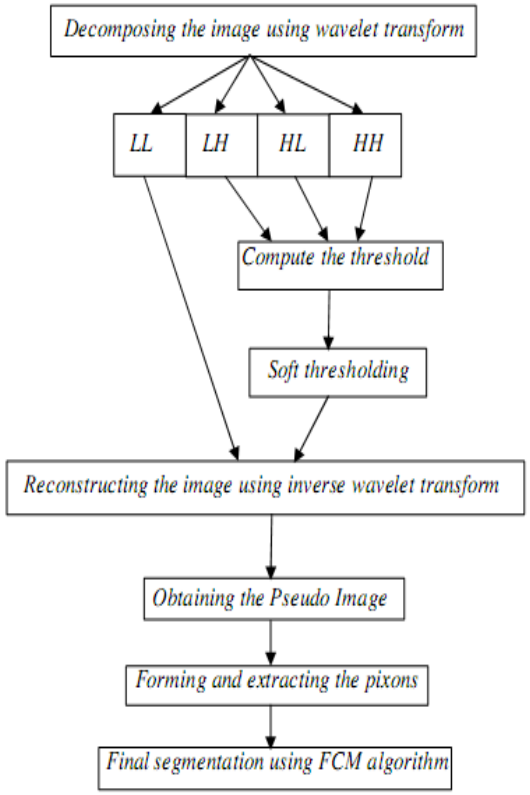

Figure 3. The block diagram of the proposed method.

a $C \times M$ matrix $U^{(0)}$. The following procedure is performed for iteration $l = 1,2,\ldots$:

1. Calculate the fuzzy cluster centers $v_c{}^l$ using $v_c = \sum_{m=1}^{M}(u_{c,m})^w x_m \,/\, \sum_{m=1}^{M}(u_{c,m})^w$.

2. Update $U^{(l)}$ using $u_{c,m} = 1/\sum_{i=1}^{C}(\frac{d_{c,m}}{d_{i,m}})^{\frac{2}{w-1}}$ where $(d_{i,m})^2 = \|x_m - v_i\|^2$ and $\|.\|$ is an inner product induced norm.

3. Compare $U^{(l)}$ with $U^{(l+1)}$ in a convenient matrix norm. If $\|U^{(l+1)} - U^{(l)}\| \le \varepsilon$ stop; otherwise continue from step 1.

The value of the weighting exponent, w determines the fuzziness of the clustering decision. A smaller value of w, i.e. w is close to unity, will give the zero/one hard decision membership function, and a larger w corresponds to a fuzzier output. Our experimental results suggest that $w = 2$ is a good choice.

Figure 3 illustrates the proposed method block diagram.

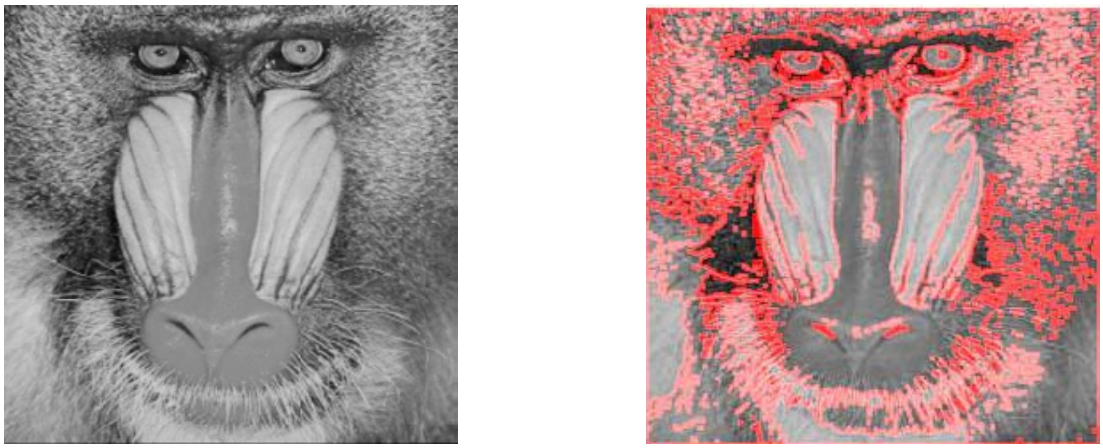

(a) (b)

Figure 4. The effect of applying the pixon forming algorithm to the Baboon image: (a) the original image, (b) the output image with boundaries between pixons.

4. EXPERIMENTAL RESULTS

In this section, first we indicate the effect of pixon forming stage on an arbitrary image. As illustrated in Fig. 4, the boundaries between the adjacent pixons are sketched so that the image segments are more proper.

The proposed segmentation method is applied on several standard images and the results of these implementations are extracted. In this section, the commonly used images such as Cortex, Baboon, and Pepper are selected and the performance of applying the proposed method on them is compared with those of two other existing approaches; Yang's method [13] and Lin's method [14]. Figs. 5(a), 6(a) and 7(a) are the Baboon, Pepper and Cortex images used in our experiment. Figs. 5(b), 6(b), 7(b) and 5(c), 6(c), 7(c) show the segmentation results of Yang's and Lin's methods, respectively. The segmentation results of our approach are illustrated in Figs. 5(d), 6(d) and 7(d). As shown in these figures, the homogeneity of regions and the discontinuity between adjacent regions, which are two main criteria in image segmentation, are enhanced in the results associated with the proposed method. In addition, several experiments have been carried out on different images and the average results are drawn in several tables. As can be seen from Table 1, the number of pixons and consequently the ratio of Pixon-Pixel in the proposed approach are decreased significantly. This is the result of applying the wavelet thresholding technique before forming pixons.

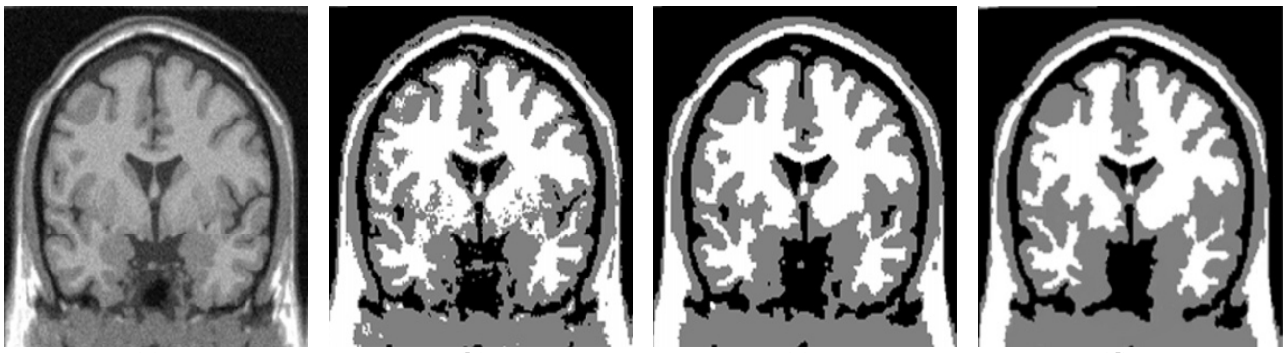

(a) (b) (c) (d)

Figure 5. Segmentation results of the Cortex image: (a) Original image, (b) Yang's method, (c) Lin's method, and (d) proposed approach.

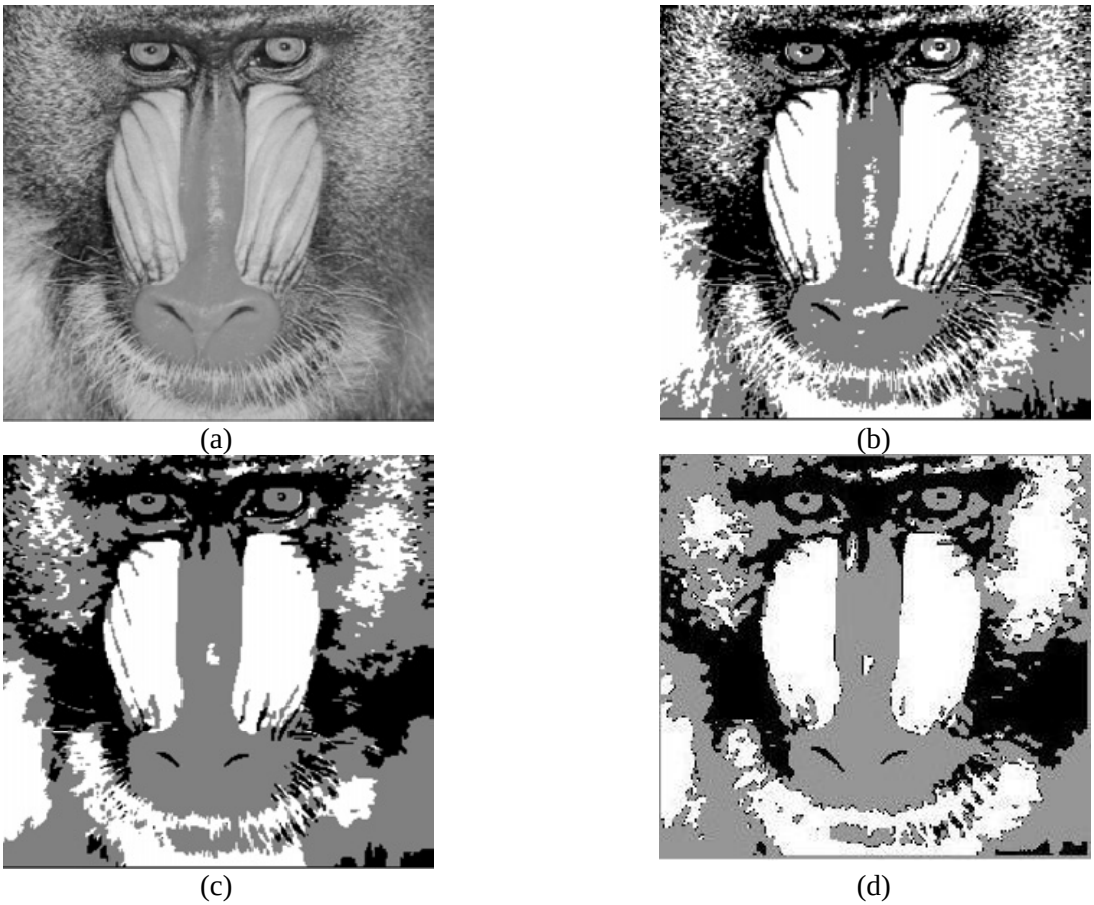

Figure 6. Segmentation results of the Baboon image: (a) Original image, (b) Yang's method, (c) Lin's method, and (d) proposed approach.

Table 2 shows the computational time required for the three methods (*computer specifications:* Intel(R) Core(TM)2 Duo CPU 2.20 GHz processor, using MATLAB 7.4). By using pixon concept with wavelet thresholding technique in our approach, the computational cost is sharply reduced. One of the most important parameters used to evaluate the performance of image segmentation methods is the variance of each segment. The smaller value of this parameter implies the more homogeneity of the region and consequently the better segmentation results. In this paper, after the segmentation process, the images are divided into three segments with possibly different average values. We have called these segments as "Classes". The variance and average of each class associated with the above-mentioned images are listed in Tables 3-5. As can be inferred from the results, the variance values for the majority of classes from different images in our method are smaller in comparison to those from the other methods. In addition to the typical variance, we calculate the normalized variance of each image after applying the three above-mentioned image segmentation approaches. If N_k and V(k) denote the number of the pixels and the variance of each class respectively, the normalized variance of each image can be determined as below:

$$V^* = \frac{V_N}{V_l} \tag{7}$$

where

$$V_N = \sum_{k=1}^{K} \frac{N_k V_k}{N} \tag{8}$$

and

$$V_l = \sum_{k=1}^{K} \frac{(I(x,y) - M)^2}{N} \tag{9}$$

In the above equations, k denotes the number of

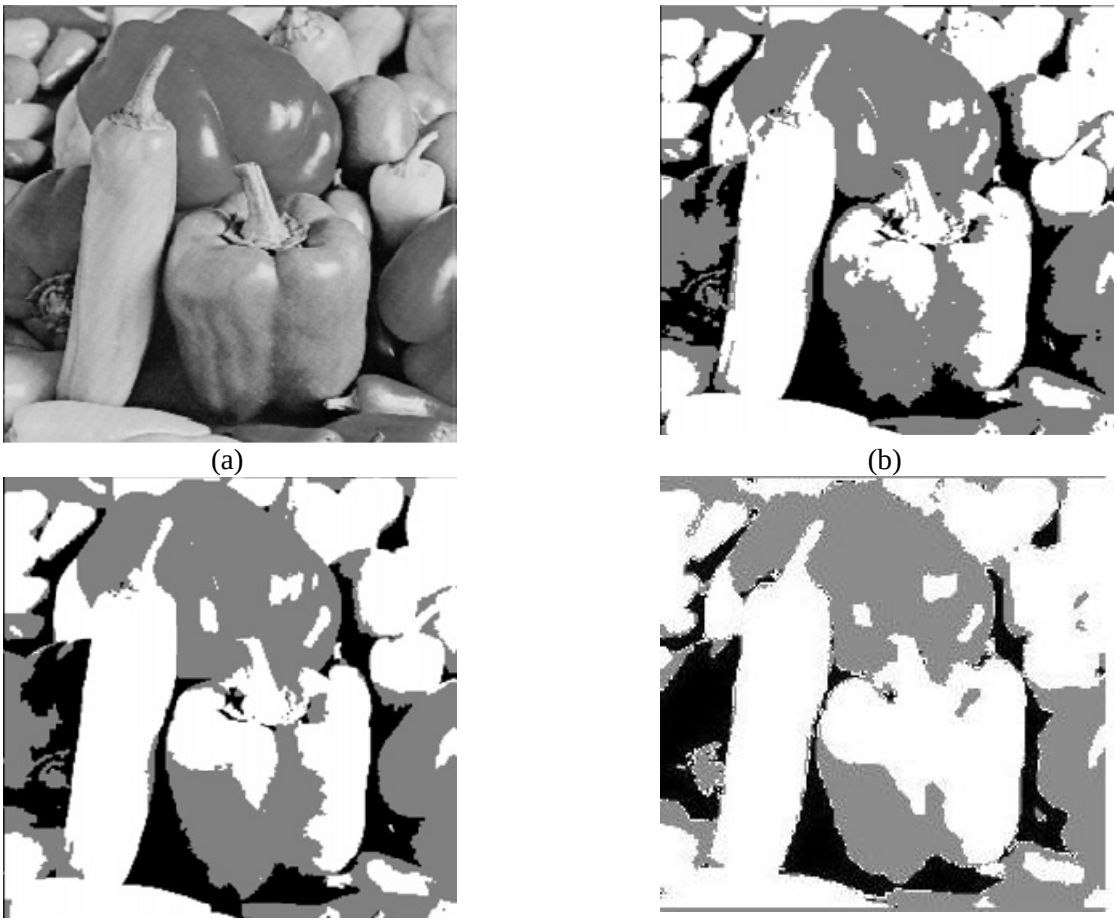

Figure 7. Segmentation results of the Pepper image: (a) Original image, (b) Yang's method, (c) Lin's method, and (d) proposed approach.

classes, $I(x,y)$ is the gray level intensity, M and N are the averaged value and the number of pixels in each image respectively. The normalized variance results illustrated in the tables demonstrate that in our approach, the amount of pixels in each cluster is closer to each other and the areas of images are more homogenous. Consequently, as can be inferred clearly from the figures, the proposed method shows a better performance in image segmentation compared to the other methods.

5. CONCLUSIONS

We have proposed an improved pixon-based method for image segmentation with utilizing the wavelet thresholding technique as a pre-processing step. Both the smoothness and uniformity of the obtained image are increased compared to the original image by using the pre-processing step. In addition, the SNR value is improved in the obtained image as the wavelet thresholding is an effective method in noise reduction. Then the pixon-representation of the image has been extracted and the Fuzzy C-Means (FCM) algorithm is successfully used to segment the image. By incorporating the pixon concept and wavelet thresholding into our method, a considerable decrement in computational costs has been achieved. If the size of image is increased, the quality of the results associated with the proposed method may not change. But the computational time of the algorithm will be certainly increased. The gained results indicate that in our technique the criteria are greatly enhanced compared to the two other well known methods and good segmentation results are obtained**.**

Table.1. Comparison of the number of pixons and the ratio between the number of pixons and pixels, among the three methods.

Images (Size)	The number of pixels	The number of pixons			The ratio between the number of pixons and pixels		
		Yang's method	Lin's method	Proposed method	Yang's method	Lin's method	Proposed method
Baboon (256×256)	262144	83362	61341	25652	31.8 %	23.4 %	9.79 %
Pepper (256×256)	262144	31981	24720	13221	12.2 %	9.43 %	5.04 %
Cortex (128×128)	16384	1819	1687	1523	11.1 %	10.2 %	9.3 %

Table.2. Comparison of the computational time, between the three methods.

Images	Yang's method (ms)	Lin's method (ms)	Proposed method(ms)
Baboon	18549	19326	15316
Pepper	16143	17034	13066
Cortex	712	697	633

Table.3. Comparison of variance values of each class, for the three algorithms (Baboon).

Method	Parameter	class 1	class 2	class 3
Yang's method	average	168.06	127.28	84.25
	variance	12.18	11.06	17.36
	Normalized Variance	**0.0279**		
Lin's method	average	167.86	126.45	82.18
	variance	12.05	11.55	16.67
	Normalized Variance	**0.0259**		
Proposed method	average	170.40	128.36	83.95
	variance	11.34	11.46	16.96
	Normalized Variance	**0.0212**		

Table.4. Comparison of variance values of each class, for the three algorithms (Pepper).

Method	Parameter	class 1	class 2	class 3
Yang's method	average	190.59	123.29	35.47
	variance	16.64	21.89	21.79
	Normalized Variance	**0.0263**		
Lin's method	average	191.68	125.27	34.39
	variance	16.28	22.66	22.30
	Normalized Variance	**0.0251**		
Proposed method	average	189.75	122.56	37.17
	variance	15.87	22.86	20.30
	Normalized Variance	**0.0217**		

Table.5. Comparison of variance values of each class, for the three algorithms. (Cortex)

Method	Parameter	class 1	class 2	class 3
Yang's method	average	22.44	93.71	197.23
	variance	12.59	11.67	14.11
	Normalized Variance	**0.0131**		
Lin's method	average	21.34	91.65	199.50
	variance	12.75	10.33	13.93
	Normalized Variance	**0.0119**		
Proposed method	average	24.25	92.49	196.72
	variance	11.37	10.51	12.81
	Normalized Variance	**0.0101**		

6. REFERENCES

1. Gonzalez, R.C. and Woods, R.E., "Digital Image Processing**"**, Prentice Hall, (2004).
2. Bonnet, N., Cutrona, J., and Herbin, M., "A 'no-threshold' histogram-based image segmentation method", ***Pattern Recognition***, Vol. 35, Issue 10, (2002), 2319-2322.
3. Shi, J. and Malik, J., "Normalized cuts and image segmentation", ***IEEE Trans. Pattern Anal. Mach. Intell.*** , Vol. 22, No 8, (2000), 888–905.
4. Zhu, S.C. and Yuille, A., "Region competition: unifying snakes, region growing, and byes/mdl for multi-band image segmentation", ***IEEE Trans. Pattern Anal.***

Mach. Intell., Vol. 18, No 9, (1996), 884–900.
5. Papamichail, G. P. and Papamichail, D.P., "The k-means range algorithm for personalized data clustering in e-commerce", ***European Journal of Operational Research***, Vol. 177, Issue 3, (2007), 1400-1408.
6. De Carvalho, F.A.T., "Fuzzy c-means clustering methods for symbolic interval data", ***Pattern Recognition Letters***, Vol. 28, Issue 4, (2007), 423-437.
7. Comaniciu, D. and Meer, P., "Mean shift: a robust approach toward feature space analysis***", IEEE Trans. Pattern Anal. Mach. Intell***., Vol. 24, No. 5, (2002), 1–18.
8. Lakshmanan, S. and Derin, H, "Simultaneous parameter estimation and segmentation of Gibbs random fields using simulated annealing", ***IEEE Trans. Pattern Anal. Machine Intell.***, Vol. 11, No. 8, (1989), 799–813.
9. Kato, Z., Zerubia, J., and Berthod, M., "Unsupervised parallel image classification using Markovian models", ***Pattern Recogniion***, Vol. 32, (1999), 591–604.
10. Elfadel, I.M. and Picard, R.W., "Gibbs random fields, cooccurrences, and texture modeling", ***IEEE Trans. Pattern Anal. Machine Intell.***,Vol. 16,(1994), 24–37.
11. Piña, R.K. and Pueter, R.C., "Bayesian image reconstruction: The pixon and optimal image modeling", ***P. A. S. P.,*** Vol. 105, (1993), 630–637.
12. Puetter, R.C., "Pixon-based multiresolution image reconstruction and the quantification of picture information content", ***Int. J. Imag. Syst. Technol***., Vol. 6, (1995), 314–331.
13. Yang, F. and Jiang, T., "Pixon-based image segmentation with Markov random fields", ***IEEE Trans. Image Process***., Vol. 12, No. 12, (2003), 1552–1559.
14. Lin, L., Zhu, L., Yang, F., and Jiang, T., "A novel pixon-representation for image segmentation based on Markov random field", ***Image and Vision Computing,*** Vol. 26, (2008), 1507–1514.
15. Donoho, D. L. and Johnstone, I.M., "Ideal spatial adaptation via wavelet shrinkage", ***Biometrika***, Vol. 81, (1994), 425-455.
16. Jansen, M., "Noise Reduction by Wavelet Thresholding", Springer Verlag New York Inc., (2001).
17. Chang, S.G., Yu, B. and Vetterli, M., "Adaptive Wavelet Thresholding for image Denoising and compression", ***IEEE Trans. Image Processing***, Vol.9, No.9, (2000), 1532-1545.
18. Gupta, S. and Kaur, L., "Wavelet Based Image Compression using Daubechies Filters", ***In proc. 8th National Conference on Communications,*** I.I.T. Bombay, (2002).
19. Burrus, C.S., Gopinath, R. A., and Guo, H., "Introduction to Wavelets and Wavelet Transforms: A Primer", New Jersey: Prentice Hall, (1998).
20. Fauzi, M.F.A. and Lewis, P.H., "A Fully Unsupervised Texture Segmentation Algorithm", ***British Machine Vision Conference***, Norwich, UK. (2003).